

Heme Levels Are Increased in Human Failing Hearts

Arineh Khechaduri, MS, Marina Bayeva, PhD, Hsiang-Chun Chang, BA, Hossein Ardehali, MD, PhD
Chicago, Illinois

- Objectives** The goal of this study was to characterize the regulation of heme and non-heme iron in human failing hearts.
- Background** Iron is an essential molecule for cellular physiology, but in excess it facilitates oxidative stress. Mitochondria are the key regulators of iron homeostasis through heme and iron-sulfur cluster synthesis. Because mitochondrial function is depressed in failing hearts and iron accumulation can lead to oxidative stress, we hypothesized that iron regulation may also be impaired in heart failure (HF).
- Methods** We measured mitochondrial and cytosolic heme and non-heme iron levels in failing human hearts retrieved during cardiac transplantation surgery. In addition, we examined the expression of genes regulating cellular iron homeostasis, the heme biosynthetic pathway, and micro-RNAs that may potentially target iron regulatory networks.
- Results** Although cytosolic non-heme iron levels were reduced in HF, mitochondrial iron content was maintained. Moreover, we observed a significant increase in heme levels in failing hearts, with corresponding feedback inhibition of the heme synthetic enzymes and no change in heme degradation. The rate-limiting enzyme in heme synthesis, delta-aminolevulinic acid synthase 2 (ALAS2), was significantly upregulated in HF. Overexpression of ALAS2 in H9c2 cardiac myoblasts resulted in increased heme levels, and hypoxia and erythropoietin treatment increased heme production through upregulation of ALAS2. Finally, increased heme levels in cardiac myoblasts were associated with excess production of reactive oxygen species and cell death, suggesting a maladaptive role for increased heme in HF.
- Conclusions** Despite global mitochondrial dysfunction, heme levels are maintained above baseline in human failing hearts. (*J Am Coll Cardiol* 2013;61:1884–93) © 2013 by the American College of Cardiology Foundation

Heart failure (HF) rates have soared over the last decade, with almost 6 million Americans affected; the prevalence of the disease is rising steadily (1). Molecular mechanisms of HF are complex (2), but mitochondrial dysfunction is an early and common finding in hypertrophied and failing hearts (3). Virtually all aspects of mitochondrial physiology are deranged in HF (4), including mitochondrial number and biogenesis (5), energetic capacity (6), and production of reactive oxygen species (ROS) (7). In addition to generating adenosine triphosphate (ATP), mitochondria play a major role in the regulation of iron balance and synthesis of heme and iron-sulfur (Fe/S) clusters (8,9); however, these processes have not been systematically examined in failing hearts.

Indirect evidence points to a link between cellular and mitochondrial iron regulation and HF. Iron is an essential molecule that functions as a cofactor in mitochondrial cytochromes, antioxidant enzymes, and more, and its deficiency is associated with cardiomyopathy (10). In contrast, the redox properties of iron make it an ideal catalyst for the production of a toxic hydroxyl radical ($\text{OH}\cdot$) by the Fenton reaction (11), and cardiac dysfunction is a prominent feature of iron overload diseases, such as hemochromatosis (12). Elevated iron levels were noted in the hearts of mice overexpressing the alpha subunit of the Gq protein, a model of cardiomyopathy (13); however, cellular distribution of iron has not been assessed. Recently, we have shown that accumulation of iron, specifically in the mitochondria through a reduction in the levels of ATP-binding cassette transporter B8 (a protein involved in mitochondrial iron export), leads to the development of cardiomyopathy in mice (14). Similarly, aggregation of iron inside the mitochondria has been observed in the hearts of Friedreich's ataxia patients (15), who develop progressive and lethal cardiac dysfunction (16). Thus, maintenance of iron balance inside the heart appears to be critical for its function, but it remains unknown how iron regulation is altered in failing human hearts.

From the Feinberg Cardiovascular Research Institute, Northwestern University School of Medicine, Chicago, Illinois. Dr. Bayeva is supported by the American Heart Association (AHA) Midwest Affiliate Predoctoral Fellowship (10PRE4430021). Dr. Ardehali is supported by the National Institutes of Health Grants (K02 HL107448, R01 HL104181, and 1P01 HL108795). Dr. Ardehali has been a member of the Speaker's Bureau for Merck and has been a consultant for Takeda, Cubist Pharma, and the Gerson Lehrman Group. All other authors have reported that they have no relationships relevant to the contents of this paper to disclose.

Manuscript received November 21, 2012; revised manuscript received January 15, 2013, accepted February 5, 2013.

Iron enters the mitochondria through an inner membrane transporter mitoferrin 2 (Mfrn2) (17,18), and can either be stored in a complex with mitoferritin (FtMt) or used in heme and Fe/S cluster biosynthetic pathways (19). Heme production begins in the mitochondria with condensation of glycine and succinyl coenzyme A to form delta-aminolevulinic acid (ALA) by the rate-limiting enzyme ALA synthase (ALAS) (9). The next 5 conversions are carried out in the cytosol. Finally, the synthesis is completed in the mitochondria with insertion of an iron atom into protoporphyrin IX (PPIX) to form heme by ferrochelatase (9) (Fig. 1). In the heart, heme functions as a catalytic or structural subunit of mitochondrial electron transport chain (ETC) complexes, myoglobin, antioxidant enzymes, and components of the cytochrome p450 (20). Moreover, heme can be broken down by heme oxygenases (HMOX) into elemental iron, carbon monoxide, and cardioprotective antioxidant biliverdin (21). Despite the essential role heme plays in the heart, this molecule remains understudied outside of the erythropoietic system.

Fe/S cluster assembly requires over 20 enzymes and scaffolding proteins, and takes place primarily in the mitochondria (8). Fe/S clusters are incorporated into mitochondrial, cytoplasmic, and nuclear proteins involved in oxidative phosphorylation, DNA repair, purine metabolism, and heme production (22,23). Disruption of Fe/S cluster synthesis may also lead to cardiomyopathy, as noted in patients with Friedreich's ataxia (24) and mice with deletion of ABCB8 (14), although these conditions are also associated with mitochondrial iron accumulation and ROS.

Given the critical role mitochondria play both in iron homeostasis and in HF, we aimed to characterize the changes in cytosolic and mitochondrial heme and non-heme iron regulation in human failing hearts. Our results demonstrate that both cytosolic and mitochondrial heme levels are increased in failing hearts, with feedback inhibition of the heme synthetic enzymes, except for ALAS2, which is increased in HF, and whose expression was previously reported to be restricted to the hematopoietic system. We also show that in H9c2 cardiac myoblasts, ALAS2 expression and heme levels are regulated by hypoxia and erythropoietin (EPO), the 2 pathways that are often altered in failing hearts. Furthermore, we demonstrate that increased heme levels are associated with elevated oxidative stress and loss of viability in cultured cardiomyoblasts.

Methods

Human samples. Tissue samples were obtained from the tissue bank at Feinberg Cardiovascular Research Institute (Northwestern University, Chicago, Illinois) and consisted of samples from nonfailing (n = 10) and failing ischemic (n = 10) human hearts. Failing ischemic tissues were obtained from the explanted hearts of cardiac transplantation recipients. Nonfailing heart tissue samples were ob-

tained from unmatched organ donors whose hearts were unsuitable for transplantation, but who had no known cardiac disease. Explanted hearts were immediately placed in cold cardioplegic solution and subsequently frozen in liquid nitrogen. Protocols for tissue procurement were approved by the Institutional Review Board of Northwestern University. Informed consent was obtained from all transplantation patients and from the families of organ donors before tissue collection.

Cell culture. H9c2 cardiac myoblasts were purchased from ATCC and kept in complete Dulbecco's Modified Eagle Medium (ATCC, Manassas, Virginia) supplemented with 10% fetal bovine serum (Invitrogen Grand Island, New York) and 1% penicillin-streptomycin. For hypoxic experiments, cells were maintained in a hypoxic chamber at 37°C and 5% carbon dioxide in the presence of 1% oxygen for up to 8 days. Medium was replaced every 2 days, and cells were collected under hypoxia before analysis. For pharmacological treatments, cells were grown to 80% to 90% confluence and incubated with 10- μ M hemin (Sigma-Aldrich, St. Louis, Missouri) and 0.6 mg/ml EPO (Sigma-Aldrich) for 48 h in complete medium.

Abbreviations and Acronyms

ALA	= delta-aminolevulinic acid
ALAS2	= ALA synthase 2
ATP	= adenosine triphosphate
ETC	= electron transport chain
EPO	= erythropoietin
Fe/S	= iron-sulfur
HF	= heart failure
HMOX1	= heme oxygenase 1
Mfrn2	= mitoferrin 2
FtMt	= mitochondrial ferritin
PCR	= polymerase chain reaction
PPIX	= protoporphyrin IX
qRT	= quantitative reverse-transcriptase
ROS	= reactive oxygen species
TfR1	= transferrin receptor 1

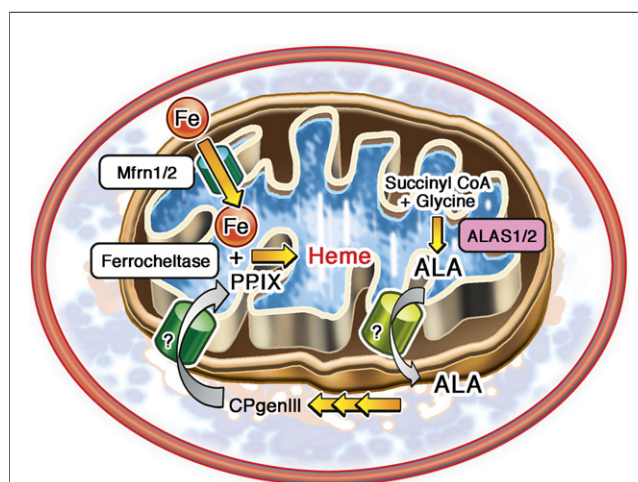


Figure 1

Schematic Representation of Cellular Heme Synthesis Pathway

ALA = delta-aminolevulinic acid; ALAS2 = ALA synthase 2; CoA = coenzyme A; CPgenIII = coproporphyrinogen III; Fe = iron; Mfrn2 = mitoferrin 2; PPIX = protoporphyrin IX.

Mitochondrial fractionation. For tissue samples, we used the Mitochondria Isolation Kit for Tissue (Pierce, Rockford, Illinois) according to the manufacturer's dounce homogenization protocol for hard tissue. Homogenized tissue was treated with reagents in the presence of ethylenediaminetetraacetic acid-free protease inhibitors (Protease Arrest, G-Biosciences, St. Louis, Missouri). To maintain the integrity of the mitochondria, samples were kept on ice during the isolation process. Following differential centrifugation at 4°C, the supernatant (cytosolic fraction) was collected, and the remaining pellet containing the mitochondria-enriched fraction was dissolved in 1% Triton X-100 (Sigma-Aldrich) in Tris-buffered saline (Cellgro, Manassas, Virginia).

Non-heme iron measurement. Mitochondrial and cytosolic non-heme iron was quantified using a commercial Iron Assay Kit (BioVision, Milpitas, California). Briefly, tissue lysate was mixed with acidic solution to release protein-bound iron, followed by a reduction of iron to its ferrous form and incubation with a Ferene S compound to produce a colored complex. The absorbance was then measured on Spectra Max Plus (Molecular Devices, Sunnyvale, California) microplate reader at 593 nm and normalized to the protein concentration of each sample.

Heme iron measurement. For determination of total heme levels, ~5 mg of frozen tissue was homogenized in 1% Triton-X100 in Tris-buffered saline and centrifuged at 5,000g for 10 min to remove debris. For determination of mitochondrial and cytosolic heme levels, the mitochondrial fraction was isolated using the Mitochondrial Isolation Kit for Tissue (Pierce) according to the manufacturer's protocol. Protein concentration of cytosolic or mitochondrial lysate was quantified by bicinchoninic acid assay (Pierce), and heme was quantified as described (25). Briefly, equal amounts of protein were mixed with 2-M oxalic acid and heated to 95°C for 30 min to release iron from heme and generate fluorescent PPIX. Samples were then centrifuged for 10 min at 1,000g at 4°C to remove debris; the fluorescence of the supernatant was assessed at 405 nm/600 nm on a Spectra Max Gemini fluorescence microplate reader and normalized to the protein concentration of each sample. For determination of unsaturated PPIX levels, incubation and heating with oxalic acid steps were omitted. Instead, samples were diluted in phosphate-buffered saline, followed by fluorescence measurement and normalization to protein content.

Knockdown and overexpression of ALAS2. For knockdown experiments, ALAS2 and control nontargeting siRNA (Thermo Scientific) were transfected into H9c2 cells using Dharmafect I reagent (Thermo Scientific, Hanover Park, Illinois) for 48 h according to the manufacturer's protocol. For hypoxia experiments, transfections were repeated every 48 h to maintain low levels of ALAS2 expression throughout the study. Knockdown efficiency was confirmed by quantitative reverse-transcriptase-polymerase chain reaction (qRT-PCR) and Western blot analyses.

ALAS2 overexpression was achieved through lentiviral transduction. Lentiviral particles coding for ALAS2-GFP fusion protein or green fluorescent protein-only control were transduced into H9c2 cells at equal multiplicity of infection for 48 h, and overexpression was confirmed by Western blotting.

Quantitative real-time PCR. RNA was isolated with RNA STAT-60 (TEL-TEST, Inc., Friendswood, Texas), reverse-transcribed with a Random Hexamer (Applied Biosystems, Foster City, California), and amplified on a 7500 Fast Real-Time PCR system with SYBR Green PCR Master Mix (Applied Biosystems). Primers were designed using Primer3 (version 0.4.0) software to target sequences spanning an exon-intron-exon boundary, and their specificity was confirmed by running a dissociation curve. mRNA levels were calculated by the comparative threshold cycle method and normalized to the beta-actin gene.

Mito-DNA/genomic DNA. Total DNA was isolated using the DNeasy Blood & Tissue Kit (Qiagen), and the ratio of cytochrome c oxidase I to the genomic 18S gene was determined by quantitative RT-PCR using SYBR Green PCR Master Mix (Applied Biosystems).

Western blot. Approximately 5 mg of tissue was homogenized in radio-immunoprecipitation assay buffer (Thermo Scientific) in the presence of Protease Arrest protease inhibitors (G-Biosciences), centrifuged at 5,000g for 15 min to remove debris and protein concentration of the supernatant determined by BCA assay. Fifteen to 30 µg of protein were resolved on sodium dodecyl sulfate polyacrylamide gel electrophoresis gels and transferred to nitrocellulose membranes (Invitrogen). The membranes were probed with antibodies against ferritin light and heavy chains (Sigma-Aldrich), HMOX1 (Abcam, Cambridge, Massachusetts), ALAS1/2 (Abcam), ferrochelatase (Proteintech), phosphor-JAK2 (Tyr1007/1008), JAK2 (Millipore, Billerica, Massachusetts), NF-E2 (Proteintech), glyceraldehyde-3-phosphate dehydrogenase (Santa Cruz), and tubulin (Abcam). Horseradish peroxidase-conjugated donkey anti-rabbit and donkey anti-mouse were used as secondary antibodies (Santa Cruz, Dallas, Texas) and visualized by Pierce SuperSignal Chemiluminescent Substrates.

Complex IV activity. Complex IV activity was determined using the Complex IV Human Enzyme Activity Microplate Assay Kit (Abcam) according to the manufacturer's protocol. Briefly, complex IV was immobilized in the wells of a 96-well plate by immunocapturing, and the specific activity was determined colorimetrically as oxidation of cytochrome c, the substrate of complex IV, by measuring absorbance change at 550 nm for 2 h at 30°C at 5-min intervals.

Mitochondrial ROS quantification. MitoSox Red (Invitrogen) was used to assess mitochondrial O₂· production (26). Cells were visualized by microscopy and ROS levels were quantified by ImageJ software (National Institutes of Health, Bethesda, Maryland). Four fields per each sample were obtained and averaged. Nuclei were counterstained with Hoescht 33342 dye (Invitrogen) and subtracted from the total

MitoSox fluorescence to exclude the signal from localization of dye into the nucleus. An accurate overlay between Hoescht and nuclear MitoSox dye was achieved by adjusting microscopy settings before data collection, with representative single-channel and overlay images presented in Online Figure 1A. In addition, total MitoSox fluorescence without nuclear signal subtraction was quantified by ImageJ.

Cell death analysis. Following ALAS2 overexpression or hemin treatment, cells were double-labeled with propidium iodide (Sigma-Aldrich) and Alexa Fluor 350-conjugated Annexin V (Molecular Probes, Eugene, Oregon), and analyzed by flow cytometry in a FACS Canto flow cytometer (BD Bioscience, San Jose, California). The data are presented as the sum of apoptotic and necrotic cells normalized to the control.

Micro-RNA experiments. Taqman micro-RNA assays (Applied Biosystems) were used to quantify miR144, 145, 148a, 148b, and 152 levels according to the manufacturer's protocol. Levels of these micro-RNAs in failing hearts were quantified by qRT-PCR and normalized to the expression of small RNA U6. To overexpress miR145, we used Pre-miR miRNA Precursors, and to downregulate miR145, we used Anti-miR miRNA Inhibitors (Ambion, Carlsbad, California). Scrambled Pre-miR and anti-scrambled Anti-miR were used in control experiments, respectively.

Statistical analysis. Data are expressed as mean \pm SEM. Statistical significance was assessed with the unpaired Student *t* test; a *p* value of <0.05 was considered statistically significant.

Results

Heme is increased in failing hearts. Mitochondria are the primary site of heme and Fe/S cluster synthesis, and their function is severely impaired in HF (Fig. 1). In this study, we characterized changes in cellular and mitochondrial iron homeostasis in failing human hearts. We used left ventricular myocardial tissue from 10 patients with terminal HF failure obtained during the heart transplantation surgery and 10 nonmyopathic hearts as controls. Consistent with mitochondrial dysfunction that is invariably present in HF (27,28), the mitochondrial DNA copy number and the activity of mitochondrial complex IV were reduced in failing hearts compared with the control hearts (Online Figs. 1B and 1C), thus providing molecular confirmation of the pathology report.

We next measured the levels of non-heme and heme iron in these hearts. There was a significant decrease in cytosolic levels of non-heme iron (Fig. 2A) and a trend toward a decrease in the levels of cytosolic iron storage protein ferritin

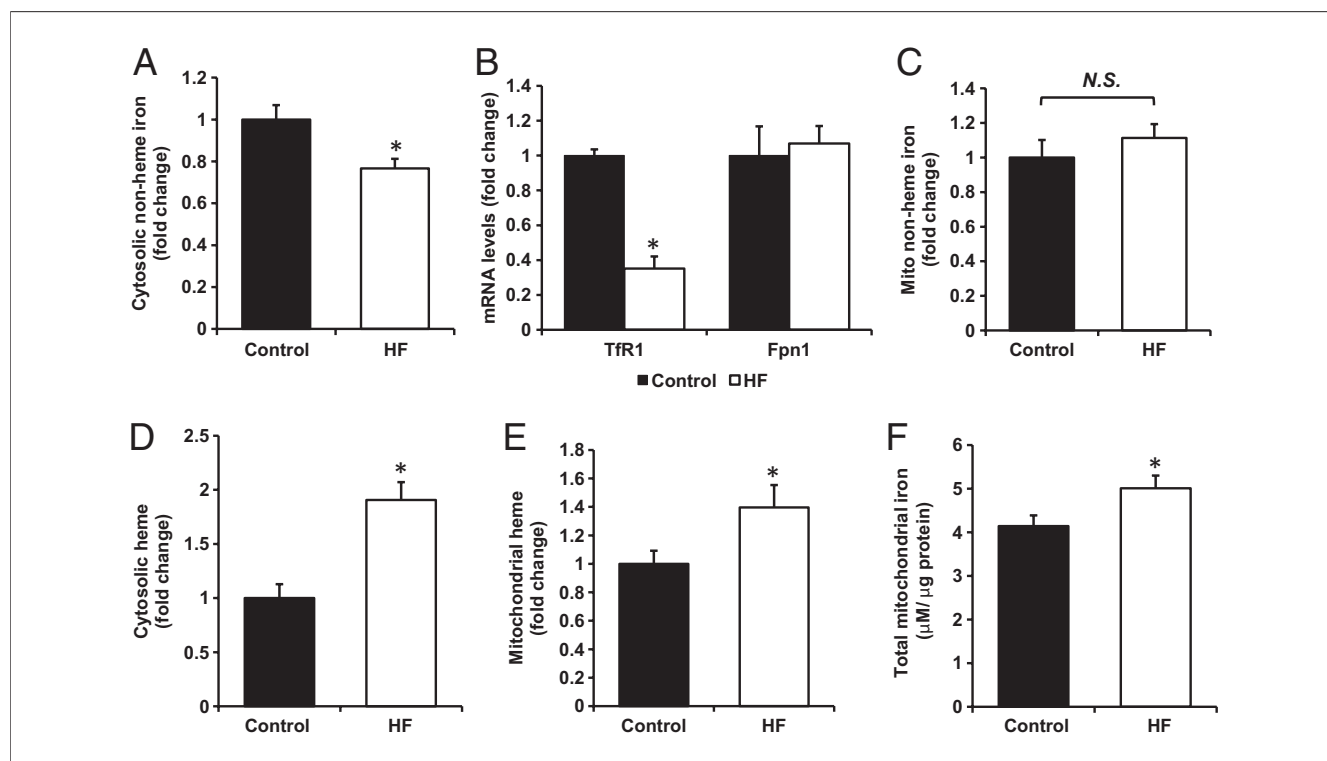


Figure 2 Heme and Non-Heme Iron Regulation in HF

(A) Cytosolic non-heme iron levels in control and failing hearts normalized to the cytosolic protein concentration (n = 10). (B) mRNA expression of transferrin receptor 1 (TfR1), an iron importer, and ferroportin 1, an iron exporter, in heart failure (HF) and control groups (n = 10). (C) Non-heme iron levels in the mitochondria of control and failing hearts normalized to mitochondrial protein content (n = 10). (D) Cytosolic and (E) mitochondrial heme levels in control and failing hearts normalized to the protein concentration of cytosolic and mitochondrial fractions, respectively (n = 10). (F) Total mitochondrial iron levels, obtained by addition of non-heme and heme iron content (n = 10). Data are presented as mean \pm SEM. **p* < 0.05 versus control group.

(heavy and light chains) (Online Figs. 2A and 2B). Moreover, mRNA levels of transferrin receptor 1 (TfR1), a protein facilitating cellular iron import, were greatly reduced, whereas the expression of ferroportin 1, an iron exporter, remained stable (Fig. 2B), suggesting that the observed deficiency may be due to a reduction in iron import in cardiomyocytes. However, mitochondrial non-heme iron content was unaltered in failing hearts (Fig. 2C), suggesting that the delivery of iron to the mitochondria remains intact in HF.

Heme levels were significantly increased in the cytosolic (Fig. 2D) and mitochondrial (Fig. 2E) fractions in failing hearts, as determined by the increase in fluorescence of the PPIX ring, the last synthetic intermediate in the heme synthesis pathway (25). The observed increase was not due to accumulation of unsaturated PPIX, because the levels of iron-free PPIX were comparable between the 2 groups (Online Fig. 2C). Thus, although mitochondrial biogenesis and energetic function are depressed in HF, mitochondrial iron levels (Fig. 2F) (obtained by the addition of heme and non-heme mitochondrial iron contents) and heme content in this organelle are increased in failing hearts.

ALAS2 expression is induced in HF. To understand the mechanism of increased heme levels in HF, we assessed the expression of genes directly involved in the breakdown or

synthesis of heme. The levels of HMOX1 and 2, the enzymes that catalyze degradation of heme, were not altered (Figs. 3A and 3B, Online Fig. 3A). These results indicate that the increase in heme levels in HF is not likely caused by impaired degradation of heme. Many of the enzymes involved in heme synthesis, including ferrochelatase responsible for iron insertion in PPIX, were actually downregulated in the failing hearts (Online Figs. 3B and 3C), suggesting a feedback inhibition on the pathway by high cellular levels of heme, as has been previously reported (9). However, mRNA and protein levels of ALAS2, a rate-limiting enzyme catalyzing the first committed step in heme synthesis (29), were significantly upregulated in the failing hearts (Figs. 3C and 3D), providing a potential mechanism for heme accumulation in HF.

The upregulation of ALAS2 in HF is surprising, because the expression of this isoform was previously reported to be restricted to a hematopoietic cell lineage, and it is not known whether upregulation of ALAS2 in the heart can affect heme levels. To test this, we conducted in vitro experiments in H9c2 cardiac myoblasts. Lentivirus-driven overexpression of human ALAS2 in H9c2 cells resulted in a ~2-fold increase in its protein levels (Fig. 3E). Consistent with our findings in human hearts, heme content was elevated in ALAS2-overexpressing cells (Fig. 3F). More-

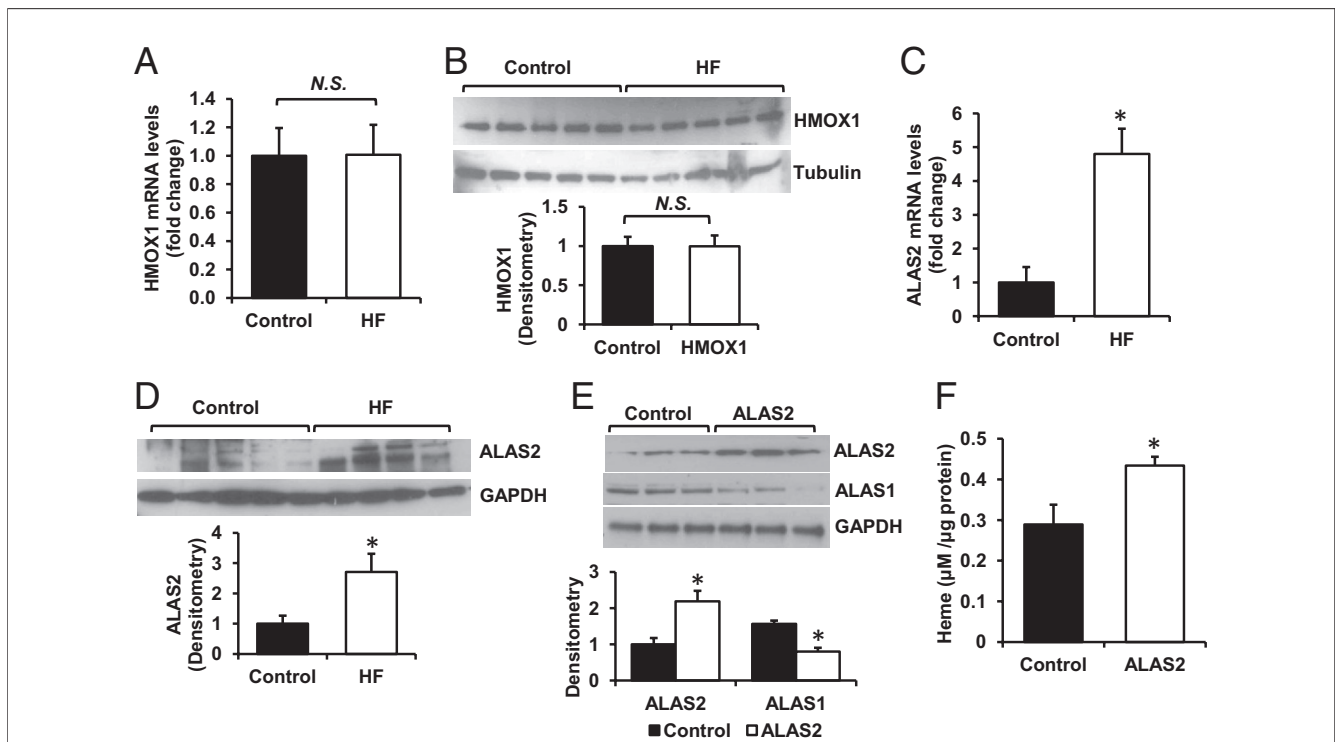


Figure 3 ALAS2 Is Upregulated in Failing Hearts

(A) mRNA and (B) protein levels of heme oxygenase 1 (HMOX1) in control and failing hearts (n = 5 to 6). (C) mRNA and (D) protein levels of ALAS2 in control and failing hearts (n = 4 to 6). (E) Western blot analysis of ALAS1/2 proteins in H9c2 with lentiviral overexpression of ALAS2 enzyme (n = 3). Densitometry analyses are presented below the Western blots. (F) Heme levels in H9c2 cells transduced with ALAS2 or control lentiviral vector (n = 6). Data are presented as mean ± SEM.

*p < 0.05 versus control group. GAPDH = glyceraldehyde-3-phosphate dehydrogenase; other abbreviations as in Figures 1 and 2.

over, mRNA and protein levels of ALAS1, the nonerthroid isoform of the enzyme, were decreased with ALAS2 over-expression (Fig. 3E, Online Fig. 3D), consistent with the feedback inhibition by high intracellular heme content (30). **Regulation of ALAS2 in cardiac cells.** Mechanisms for regulation of ALAS2 in hematopoietic cells have been extensively characterized, but it is unknown how ALAS2 is regulated in the heart. The major inducer of ALAS2 in developing erythrocytes is the GATA1 transcription factor. However, qRT-PCR analysis revealed no expression of GATA1 in human hearts (qRT-PCR cycle 34.85 ± 0.32). In contrast, protein levels of NF-E2, an erythroid transcription factor that has putative binding sites in the promoter of ALAS2 (31), were significantly higher in the HF group compared with the control group (Online Figs. 4A and 4B).

Because ischemia is common in failing hearts, and ALAS2 was shown to be regulated by hypoxia-inducible factor 1- α in erythroid lineage (32), we assessed regulation of ALAS2 by low oxygen tension by subjecting H9c2 cells to 1% oxygen levels. We found ALAS2 expression to be significantly induced by long-term (8 day), but not acute exposure, to hypoxia (Figs. 4A and 4B), with a corresponding increase in cellular heme content at day 8 (Fig. 4C). Treatment of cells with ALAS2 siRNA during hypoxic incubation effectively ablated an

increase in ALAS2 mRNA levels, bringing it down to the normoxic levels (Figs. 4D and 4E), and also prevented the increase in cellular heme (Fig. 4F). These data suggest that long-standing ischemia of failing hearts may potentially be responsible for the induction of ALAS2, and provide further evidence that upregulation of ALAS2 in HF may mediate the increase in heme levels.

Finally, ALAS2 is known to be positively regulated by EPO in erythroblasts (33), and EPO levels are often elevated in HF patients due to underlying anemia (34). The EPO receptor was previously shown to be expressed in the human heart (35), suggesting that cardiomyocytes may respond to EPO signaling. Western blot analysis of JAK2 kinase, the downstream effector of EPO signaling (36), revealed that elevated phosphorylation of this protein was consistent with activation of the EPO receptor (Fig. 5A). Incubation of H9c2 myoblasts with EPO also significantly increased p-JAK2 levels (Fig. 5B) and was associated with induction of the ALAS2 enzyme on mRNA and protein levels (Figs. 5B and 5C). Heme content was increased in EPO-treated cells (Fig. 5D), whereas suppression of ALAS2 upregulation by EPO using siRNA reversed this increase (Figs. 5E and 5F). Thus, similar to erythropoietic cells, cardiac ALAS2 is responsive to EPO stimulation, which causes an increase in heme levels and may potentially contribute to cardiac heme loading in HF, particularly in the

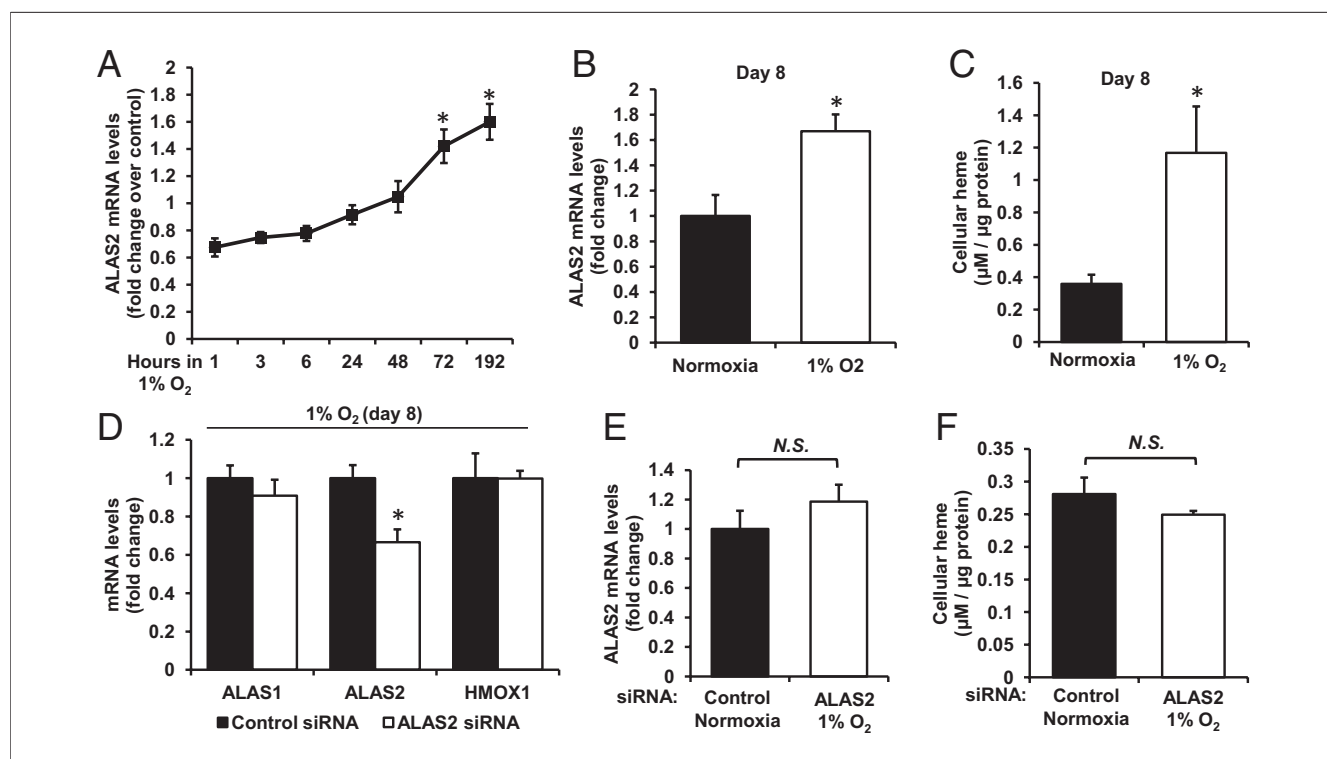


Figure 4 Regulation of ALAS2 by Hypoxia in Cardiac Myoblasts

(A) Time-course of ALAS2 mRNA expression in H9c2 cardiac myoblasts subjected to hypoxia (n = 6). (B) ALAS2 mRNA levels after 8 days in hypoxia or normoxia (n = 6). (C) Cellular heme content after 8 days in hypoxia or normoxia (n = 6). (D) mRNA levels of heme synthesis/degradation enzymes in hypoxic cardiac myoblasts with or without siRNA-mediated ALAS2 knockdown (n = 6). (E) Comparison of ALAS2 mRNA levels in control normoxic and ALAS2 siRNA-treated hypoxic cells after 8 days (n = 6). (F) Heme levels in control normoxic and ALAS2 siRNA hypoxic cells after 8 days (n = 6). Data are presented as mean \pm SEM. *p < 0.05 versus control group. Abbreviations as in Figure 1.

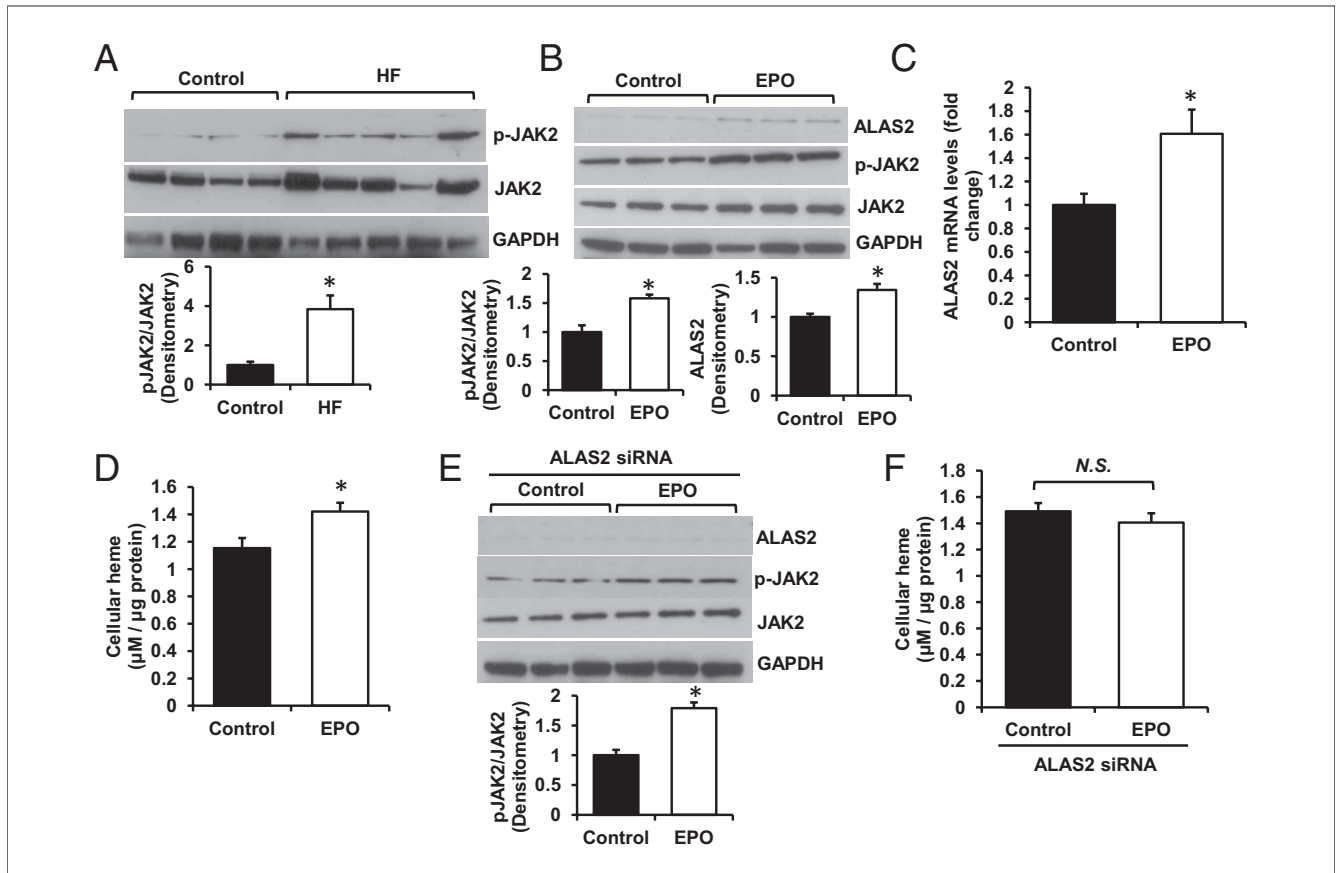


Figure 5 ALAS2 Is Regulated by Erythropoietin

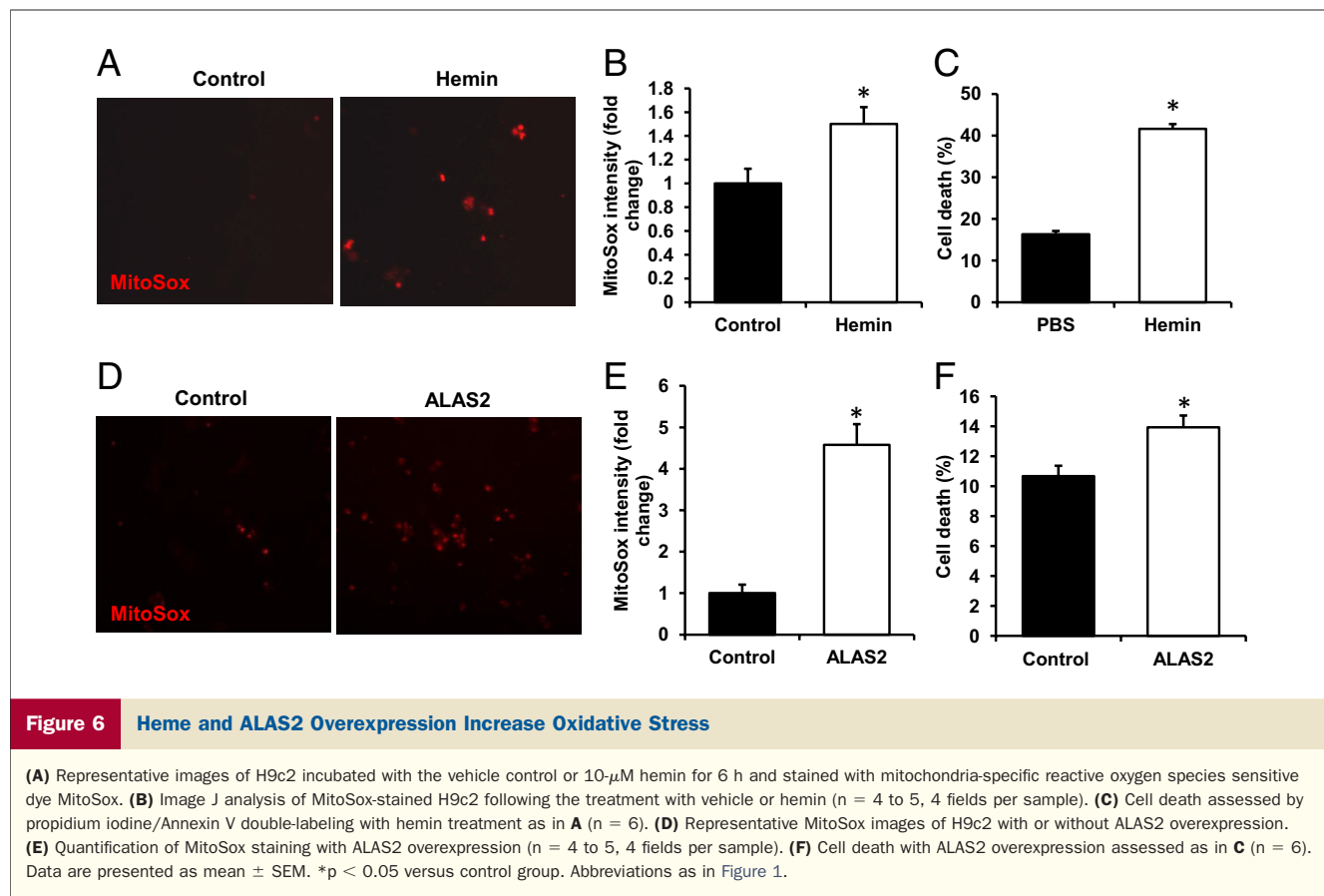
(A) Western blot analysis of p-JAK2 and JAK2 protein in failing and control hearts (n = 4 to 5). (B) ALAS2 and pJAK2/JAK2 protein levels in H9c2 cells treated with 0.6 mg/ml erythropoietin (EPO) (n = 3). (C) Quantitative reverse-transcriptase-polymerase chain reaction analysis of ALAS2 mRNA expression in H9c2 cells with EPO or vehicle control treatment (n = 6). (D) Cellular heme content with EPO treatment in cardiac myoblasts (n = 6). (E) Western blot analysis of ALAS2 and pJAK2/JAK2 in ALAS2 siRNA-treated cells incubated with EPO or vehicle control (n = 3). (F) Cellular heme content in EPO- or vehicle-treated cells with ALAS2 siRNA knockdown (n = 6). Data are presented as mean ± SEM. *p < 0.05 versus control group. Abbreviations as in Figures 1 and 3.

setting of underlying anemia. In summary, we found ALAS2 to be positively regulated by hypoxia and EPO in cardiac cells.

Heme and oxidative stress. Heart failure is characterized by increased oxidative stress, which significantly disrupts myocardial architecture and signaling (37). Free heme has been suggested to exert toxic effects through oxidation of phospholipids, mtDNA damage, and activation of the inflammatory response (38). To determine if excess levels of heme contribute to oxidative stress in cardiac myoblasts, we incubated H9c2 cells with hemin and measured mitochondrial ROS production and cell death using MitoSox and propidium iodine staining, respectively. Addition of hemin led to a significant increase in ROS levels (Figs. 6A and 6B, Online Fig. 4C) and was associated with the loss of cell viability (Fig. 6C). Overexpression of ALAS2 in H9c2 also induced an increase in ROS (Figs. 6D and 6E, Online Fig. 4D) and was associated with increased cell death (Fig. 6F). These data suggest that elevated heme production in HF may be maladaptive through enhancing oxidative stress in these hearts.

MiR-145 does not regulate iron homeostasis in HF. Micro-RNA are small noncoding RNA molecules that regulate expression of multiple genes by targeting their 3' untranslated regions (39). We and others have shown that HF is associated with reduced levels of TfR1, the protein responsible for iron uptake by cardiomyocytes (40). To determine if suppression of TfR1 in HF is mediated by a micro-RNA, we screened the 3' untranslated regions of TfR1 for putative miR target sequences and the expression of these micro-RNAs was determined using qRT-PCR (Online Fig. 5A). A significant upregulation of miR-145 was noted in the failing hearts (Online Fig. 5A).

To determine if miR-145 is responsible for the changes in iron homeostasis observed earlier, we overexpressed (Online Fig. 5B) and downregulated (Online Fig. 5C) this miR in H9c2 cardiac myoblasts, followed by the measurement of heme and non-heme iron levels. However, neither of the interventions led to significant changes in heme and non-heme iron content (Online Figs. 5D to 5G). To determine if miR-145 expression was induced secondarily to the elevated heme levels, we treated H9c2 cells with



ALA, the rate-limiting intermediate in the heme synthesis pathway, and observed a significant increase in heme levels (Online Fig. 5H), but no change in miR145 expression (Online Fig. 5I). Taken together, these results showed that although miR-145 is significantly upregulated in the failing hearts, it does not mediate changes in heme and non-heme iron homeostasis observed in HF and is not regulated by cellular heme levels.

Discussion

The goal of this study was to characterize changes in iron homeostasis occurring in failing human hearts. Despite mitochondrial dysfunction, which is characteristic of HF, the mitochondria-dependent process of heme synthesis was significantly upregulated in failing hearts. We also observed induction of ALAS2, a rate-limiting enzyme in heme synthesis that was previously reported to be expressed exclusively in hematopoietic cells. Moreover, mitochondrial iron levels were maintained at normal levels and were sufficient to support heme synthesis, because we detected very low levels of unsaturated PPIX in the HF group.

It is presently unclear whether the increase in heme levels in HF is an adaptive or maladaptive process. Heme degradation by HMOX1 confers cardiac protection through generation of an antioxidant, biliverdin, and an anti-

inflammatory molecule of carbon monoxide (29). Induction of HMOX1 was found to be beneficial in HF (41,42). However, free heme is toxic to the cell because it catalyzes oxidation and breakdown of proteins and DNA, intercalates into lipid bilayers, and damages membrane-bound organelles (38). Similarly, we found that treatment of cardiac myoblasts with hemin significantly elevated ROS generation in the mitochondria and led to a loss in cell viability. Similarly, overexpression of ALAS2, which increases heme content in H9c2 cells, increased both ROS and cell death. In contrast, the levels of HMOX1 were unaltered in the HF samples we examined, suggesting that HMOX1-dependent antioxidation is unlikely to protect hearts from heme toxicity. Based on the *in vitro* data, we speculated that the induction of heme synthesis in these hearts might be maladaptive through an increase in oxidative stress. Although our data suggested that iron supplementation and stimulants of EPO in anemic HF patients, which yielded controversial results (43), might negatively affect cardiomyocytes through induction of ALAS2 and heme synthesis, potential benefits of iron supplementation, as previously demonstrated (44), on other organs and the hematopoietic system could not be excluded. It is important to note, however, that our data only provided an association among induction of ALAS2, elevated cardiac heme levels, and HF. Generation of a cardiac-specific

ALAS2-overexpressing mouse model would allow testing of this hypothesis directly.

Although our experimental design does not identify the mechanism for increased heme synthesis and ALAS2 induction, we hypothesize that chronic ischemia and EPO may play a role. Two isoforms of ALAS enzyme have been identified. ALAS1 is a ubiquitously expressed housekeeping gene and is negatively regulated by heme (45,46). In contrast, ALAS2 expression is traditionally studied in the context of erythrocyte maturation, where it is induced to stimulate hemoglobinization (47,48). Unlike other components of the heme synthesis pathway, including ALAS1, ALAS2 is not inhibited by high levels of heme and is positively regulated by hypoxia (32,49). Our studies show that ALAS2 is expressed in the heart and is significantly upregulated in HF, providing the first evidence of a heart-specific function for this “noncardiac” isoform of ALAS. We confirm that, similar to erythroid cells, ALAS2 is regulated by hypoxia in cardiac myoblasts, and that the increase in heme observed in cells subjected to long-term hypoxia is mediated by ALAS2 induction, because knock-down of this protein has also abolished an increase in heme. Moreover, we find that, similar to developing erythrocytes, EPO stimulation induces ALAS2 expression and subsequently elevates heme levels. The significance of these findings in the context of failing hearts remains to be determined. Despite elevated EPO levels, HF patients were found to be resistant to EPO signaling in promoting hematopoiesis (34), but it remains unknown whether the sensitivity of cardiomyocytes to EPO stimulation is also altered.

In addition to showing an increase in heme content in HF, we find that miR-145 is strongly induced in failing human hearts, but it does not mediate the changes in heme observed in HF. MiR-145 is known to play a role in smooth muscle differentiation (50,51) and also exhibits tumor suppressor activity (52,53). To the best of our knowledge, this is the first report of miR145 upregulation in HF, and naturally, it will be of interest to see if this induction has any functional consequences.

We show that mitochondrial iron levels are increased in failing hearts due to an increase in heme content, suggesting that mitochondrial iron homeostasis is maintained despite severe mitochondrial dysfunction. We would like to note, however, that preservation of mitochondrial iron content does not necessarily imply that all iron-dependent processes remain unaffected. Specifically, it remains to be determined how HF affects the process of Fe/S cluster assembly in the mitochondria and their incorporation into proteins. Fe/S clusters are essential for maintenance of normal energy homeostasis, because they are required for the function of several subunits of ETC complexes and the tricarboxylic cycle enzyme aconitase. We and others report reduced activity of ETC complexes and aconitase in HF, suggesting that Fe/S cluster biosynthesis may be disrupted in failing hearts (54).

Study limitations. The potential limitations of our studies include the lack of data on demographics, the underlying cause of HF, and/or medical therapy received by patients before the transplantation surgery and retrieval of the heart. Likely, our samples come from a heterogeneous patient population. The effects of medications, methods for preservation, and ischemic time for both control and failing hearts are important factors that may have affected the reported findings. Finally, the mechanisms of cellular iron regulation are complex and multiple. Thus, unmeasured confounders may potentially contribute to the presented findings.

Conclusions

In this study we report increased myocardial heme levels in human failing hearts. While the exact mechanism and pathologic significance of this finding requires further investigation, hypoxia- or erythropoietin-driven upregulation of ALAS2 may play a role. In summary, our data suggest that induction heme synthesis pathway represents a common and important pathophysiologic finding in HF.

Acknowledgments

The authors are grateful to all members of Feinberg Cardiovascular Research Institute for insightful comments and support.

Reprint requests and correspondence: Dr. Hossein Ardehali, Northwestern University Medical Center, Feinberg Cardiovascular Research Institute, Tarry 14-733, 303 East Chicago Avenue, Chicago, Illinois 60611. E-mail: h-ardehali@northwestern.edu.

REFERENCES

1. Lloyd-Jones D, Adams RJ, Brown TM, Carnethon M, et al. Heart disease and stroke statistics—2010 update: a report from the American Heart Association. *Circulation* 2010;121:e46–215.
2. Mudd JO, Kass DA. Tackling heart failure in the twenty-first century. *Nature* 2008;451:919–28.
3. Karamanlidis G, Bautista-Hernandez V, Fynn-Thompson F, et al. Impaired mitochondrial biogenesis precedes heart failure in right ventricular hypertrophy in congenital heart disease. *Circ Heart Fail* 2011;4:707–13.
4. Bayeva M, Gheorghiadu M, Ardehali H. Mitochondria as therapeutic target in heart failure. *J Am Coll Cardiol* 2013;61:599–610.
5. Sihag S, Cresci S, Li AY, Sucharov CC, et al. PGC-1 α and ERR α target gene downregulation is a signature of the failing human heart. *J Mol Cell Cardiol* 2009;46:201–12.
6. Ventura-Clapier R, Garnier A, Veksler V, Joubert F. Bioenergetics of the failing heart. *Biochim Biophys Acta* 2011;1813:1360–72.
7. Tsutsui H, Kinugawa S, Matsushima S. Oxidative stress and mitochondrial DNA damage in heart failure. *Circ J* 2008;72 Suppl A:A31–7.
8. Lill R, Hoffmann B, Molik S, Pierik AJ, et al. The role of mitochondria in cellular iron-sulfur protein biogenesis and iron metabolism. *Biochim Biophys Acta* 2012;1823:1491–508.
9. Khan AA, Quigley JG. Control of intracellular heme levels: heme transporters and heme oxygenases. *Biochim Biophys Acta* 2011;1813:668–82.
10. Hegde N, Rich MW, Gayomali C. The cardiomyopathy of iron deficiency. *Tex Heart Inst J* 2006;33:340–4.
11. Aisen P, Enns C, Wessling-Resnick M. Chemistry and biology of eukaryotic iron metabolism. *Int J Biochem Cell Biol* 2001;33:940–59.

12. Kohgo Y, Ikuta K, Ohtake T, Torimoto Y, et al. Body iron metabolism and pathophysiology of iron overload. *Int J Hematol* 2008;88:7–15.
13. Elas M, Bielanska J, Pustelny K, et al. Detection of mitochondrial dysfunction by EPR technique in mouse model of dilated cardiomyopathy. *Free Radic Biol Med* 2008;45:321–8.
14. Ichikawa Y, Bayeva M, Ghanefar M, et al. Disruption of ATP-binding cassette B8 in mice leads to cardiomyopathy through a decrease in mitochondrial iron export. *Proc Natl Acad Sci U S A* 2012;109:4152–7.
15. Michael S, Petrocine SV, Qian J, et al. Iron and iron-responsive proteins in the cardiomyopathy of Friedreich's ataxia. *Cerebellum* 2006;5:257–67.
16. Payne RM. The heart in Friedreich's ataxia: basic findings and clinical implications. *Prog Pediatr Cardiol* 2011;31:103–9.
17. Shaw GC, Cope JJ, Li L, Corson K, et al. Mitoferrin is essential for erythroid iron assimilation. *Nature* 2006;440:96–100.
18. Paradkar PN, Zumbrennen KB, Paw BH, Ward DM, et al. Regulation of mitochondrial iron import through differential turnover of mitoferrin 1 and mitoferrin 2. *Mol Cell Biol* 2009;29:1007–16.
19. Wang J, Pantopoulos K. Regulation of cellular iron metabolism. *Biochem J* 2011;434:365–81.
20. Furuyama K, Kaneko K, Vargas PD. Heme as a magnificent molecule with multiple missions: heme determines its own fate and governs cellular homeostasis. *Tohoku J Exp Med* 2007;213:1–16.
21. Wu ML, Ho YC, Lin CY, Yet SF. Heme oxygenase-1 in inflammation and cardiovascular disease. *Am J Cardiovasc Dis* 2011;1:150–8.
22. Rouault TA, Tong WH. Iron-sulphur cluster biogenesis and mitochondrial iron homeostasis. *Nat Rev Mol Cell Biol* 2005;6:345–51.
23. Hausmann A, Samans B, Lill R, Muhlenhoff U. Cellular and mitochondrial remodeling upon defects in iron-sulfur protein biogenesis. *J Biol Chem* 2008;283:8318–30.
24. Napier I, Ponka P, Richardson DR. Iron trafficking in the mitochondrion: novel pathways revealed by disease. *Blood* 2005;105:1867–74.
25. Ward JH, Jordan I, Kushner JP, Kaplan J. Heme regulation of HeLa cell transferrin receptor number. *J Biol Chem* 1984;259:13235–40.
26. Gordon LI, Burke MA, Singh AT, et al. Blockade of the erbB2 receptor induces cardiomyocyte death through mitochondrial and reactive oxygen species-dependent pathways. *J Biol Chem* 2009;284:2080–7.
27. Ide T, Tsutsui H, Hayashidani S, et al. Mitochondrial DNA damage and dysfunction associated with oxidative stress in failing hearts after myocardial infarction. *Circ Res* 2001;88:529–35.
28. Marin-Garcia J, Goldenthal MJ, Pierpont ME, Ananthkrishnan R. Impaired mitochondrial function in idiopathic dilated cardiomyopathy: biochemical and molecular analysis. *J Card Fail* 1995;1:285–91.
29. Rytter SW, Tyrrell RM. The heme synthesis and degradation pathways: role in oxidant sensitivity. Heme oxygenase has both pro- and antioxidant properties. *Free Radic Biol Med* 2000;28:289–309.
30. Gotoh S, Nakamura T, Kataoka T, Taketani S. Egr-1 regulates the transcriptional repression of mouse delta-aminolevulinic acid synthase 1 by heme. *Gene* 2011;472:28–36.
31. Kramer MF, Gunaratne P, Ferreira GC. Transcriptional regulation of the murine erythroid-specific 5-aminolevulinic acid synthase gene. *Gene* 2000;247:153–66.
32. Zhang FL, Shen GM, Liu XL, et al. Hypoxic induction of human erythroid-specific delta-aminolevulinic acid synthase mediated by hypoxia-inducible factor 1. *Biochemistry* 2011;50:1194–202.
33. Sadlon TJ, Dell'Oso T, Surinya KH, May BK. Regulation of erythroid 5-aminolevulinic acid synthase expression during erythropoiesis. *Int J Biochem Cell Biol* 1999;31:1153–67.
34. Okonko DO, Marley SB, Anker SD, et al. Suppression of erythropoiesis in patients with chronic heart failure and anaemia of unknown origin: evidence of an immune basis. *Int J Cardiol* 2011 [E-pub ahead of print]; <http://dx.doi.org/10.1016/j.ijcard.2011.11.081>.
35. Depping R, Kawakami K, Ocker H, et al. Expression of the erythropoietin receptor in human heart. *J Thorac Cardiovasc Surg* 2005;130:877–8.
36. Witthuhn BA, Quelle FW, Silvennoinen O, et al. JAK2 associates with the erythropoietin receptor and is tyrosine phosphorylated and activated following stimulation with erythropoietin. *Cell* 1993;74:227–36.
37. Tsutsui H, Kinugawa S, Matsushima S. Oxidative stress and heart failure. *Am J Physiol Heart Circ Physiol* 2011;301:H2181–90.
38. Kumar S, Bandyopadhyay U. Free heme toxicity and its detoxification systems in humans. *Toxicol Lett* 2005;157:175–88.
39. Filipowicz W, Bhattacharyya SN, Sonenberg N. Mechanisms of post-transcriptional regulation by microRNAs: are the answers in sight? *Nat Rev Genet* 2008;9:102–14.
40. Maeder MT, Khammy O, dos Remedios C, Kaye DM. Myocardial and systemic iron depletion in heart failure implications for anemia accompanying heart failure. *J Am Coll Cardiol* 2011;58:474–80.
41. Lakkisto P, Siren JM, Kyto V, et al. Heme oxygenase-1 induction protects the heart and modulates cellular and extracellular remodeling after myocardial infarction in rats. *Exp Biol Med (Maywood)* 2011;236:1437–48.
42. Wu ML, Ho YC, Yet SF. A central role of heme oxygenase-1 in cardiovascular protection. *Antioxid Redox Signal* 2011;15:1835–46.
43. van Veldhuisen DJ, Anker SD, Ponikowski P, Macdougall IC. Anemia and iron deficiency in heart failure: mechanisms and therapeutic approaches. *Nat Rev Cardiol* 2011;8:485–93.
44. Anker SD, Comin Colet J, Filippatos G, et al. Ferric carboxymaltose in patients with heart failure and iron deficiency. *N Engl J Med* 2009;361:2436–48.
45. Yoshino K, Munakata H, Kuge O, Ito et al. Haeme-regulated degradation of delta-aminolevulinic acid synthase 1 in rat liver mitochondria. *J Biochem* 2007;142:453–8.
46. Zheng J, Shan Y, Lambrecht RW, et al. Differential regulation of human ALAS1 mRNA and protein levels by heme and cobalt protoporphyrin. *Mol Cell Biochem* 2008;319:153–61.
47. May BK, Dogra SC, Sadlon TJ, et al. Molecular regulation of heme biosynthesis in higher vertebrates. *Prog Nucleic Acid Res Mol Biol* 1995;51:1–51.
48. Cox TC, Sadlon TJ, Schwarz QP, Matthews CS, et al. The major splice variant of human 5-aminolevulinic acid synthase-2 contributes significantly to erythroid heme biosynthesis. *Int J Biochem Cell Biol* 2004;36:281–95.
49. Kaneko K, Furuyama K, Aburatani H, Shibahara S. Hypoxia induces erythroid-specific 5-aminolevulinic acid synthase expression in human erythroid cells through transforming growth factor-beta signaling. *FEBS J* 2009;276:1370–82.
50. Yamaguchi S, Yamahara K, Homma K, Suzuki S, et al. The role of microRNA-145 in human embryonic stem cell differentiation into vascular cells. *Atherosclerosis* 2011;219:468–74.
51. Rangrez AY, Massy ZA, Metzinger-Le Meuth V, Metzinger L. miR-143 and miR-145: molecular keys to switch the phenotype of vascular smooth muscle cells. *Circ Cardiovasc Genet* 2011;4:197–205.
52. Chen X, Gong J, Zeng H, Chen N, et al. MicroRNA145 targets BNIP3 and suppresses prostate cancer progression. *Cancer Res* 2010;70:2728–38.
53. La Rocca G, Badin M, Shi B, et al. Mechanism of growth inhibition by MicroRNA 145: the role of the IGF-I receptor signaling pathway. *J Cell Physiol* 2009;220:485–91.
54. Qanud K, Mamdani M, Pepe M, et al. Reverse changes in cardiac substrate oxidation in dogs recovering from heart failure. *Am J Physiol Heart Circ Physiol* 2008;295:H2098–105.

Key Words: ALAS2 ■ heart failure ■ heme ■ iron ■ mitochondria.

 **APPENDIX**

For supplemental figures, please see the online version of this article.